Research Article Vol. 56, No. 24 / August 20 2017 / Applied Optics 6949

applied optics

Compressive correlation holography

Rachit Saluja,[1,2] G. R. K. S. Subrahmanyam,[3] Deepak Mishra,[1,*] R. V. Vinu,[2] and Rakesh Kumar Singh[2]

[1]Department of Avionics, Indian Institute of Space Science and Technology (IIST), Trivandrum, 695547 Kerala, India
[2]Applied and Adaptive Optics Laboratory, Department of Physics, Indian Institute of Space Science and Technology (IIST), Trivandrum, 695547 Kerala, India
[3]Department of Electrical Engineering, Indian Institute of Technology Tirupati, Andhra Pradesh 517506, India
*Corresponding author: deepak.mishra@iist.ac.in

Received 22 May 2017; revised 22 July 2017; accepted 24 July 2017; posted 24 July 2017 (Doc. ID 295419); published 17 August 2017

We propose and demonstrate a compressive sensing (CS) framework for correlation holography. This is accomplished by adopting the principle of compressive sensing and thresholding in the two-point intensity correlation. The measurement matrix and the sensing matrix that are required for applying the CS framework here are systematically extracted from the random illuminations of the laser speckle data. Reconstruction results using CS, CS with thresholding, and intensity correlation are compared. Our study reveals that liminal CS requires far fewer samples for the reconstruction of the hologram and has wide application in image reconstruction.

OCIS codes: (090.0090) Holography; (100.3010) Image reconstruction techniques; (110.0113) Imaging through turbid media; (070.2025) Discrete optical signal processing.

https://doi.org/10.1364/AO.56.006949

1. INTRODUCTION

Holography allows recording and reconstruction of the complex field of the light. With the advent of digital holography (DH), several significant advantages, such as full-field imaging, nondestructive imaging, and digital propagation of the field without mechanical focusing, have been demonstrated [1]. When the object is obscured by the diffuser, the direct recording and reconstruction of the object information by conventional holography is difficult or impossible due inhomogeneous scattering. Random scattering diffuses the field information of the object into a highly disordered complex speckle pattern. Several techniques that use correlation of the random field are proposed to overcome such a situation [2–13]. Among many, the correlation holography is recently proposed to reconstruct complex information of the object as the distribution of the correlation structure of the random field [9–12]. It is common practice to replace the ensemble average with temporal (or spatial) averaging, assuming ergodicity in time or space, in experimental implementation of correlation imaging [13–15]. This is carried out by the pseudothermal sources or spatially random fields. However, realization with pseudothermal sources requires long capturing time for reconstruction of the images with a good signal-to-noise ratio. Similarly, the requirement of being wide-sense stationary in space for the spatial averaging brings strict requirements on the experimental realization.

Recently, the application of the compressive sensing theory has been successfully demonstrated in astronomy, terahertz imaging, holography, ghost imaging, and lidar [16–24]. The implementation of the compressed sensing approach in astronomy provides an elegant and effective compression technique that can overcome the compression issues faced in astronomical data processing [16]. A Fourier imaging system with compressed sensing is demonstrated using significantly fewer measurements than a conventional imaging technique, and the technique has potential applications in terahertz imaging [17]. In recent years, significant numbers of works were successfully demonstrated with CS in holography, and this has resulted in wide applications in 3D tomography and compressive digital holographic sensing applications [18,19]. CS theory, in combination with ghost imaging, is effectively employed to boost the recovered image quality and it enables the image reconstruction with far less data compared with conventional ghost imaging [20–22]. A potential application of this is the development of a ghost imaging lidar system in the area of remote imaging [23]. Recently, compressed correlation with random illumination has demonstrated that it is possible to achieve superior imaging capabilities with less computational burden [24].

Despite the fact that the implementation of CS theory is executed in different imaging scenarios, the idea has not been applied in the correlation holography techniques, which have attracted significant attention in recent years due to their 3D imaging capability and complex field imaging [9–15]. Correlation-holography-based imaging techniques require a

large number of random samples in order to implement the ensemble averaging, and this makes for experimental or computational complexity. This is realized either by exploiting temporal (or spatial) ergodicity. In this work, we demonstrate the ability of compressive sensing to reconstruct the object using far fewer random samples than the conventional correlation holography, and this can be applied for both temporal and spatial fluctuating fields. We make use of spatial averaging (rather than temporal) as a replacement for the ensemble averaging. One direct outcome of this approach is reduction in the demand of detecting the random field with large array of detectors for faithful recovery of the object. We adopt compressive sensing theory and thresholding in the two-point intensity correlation and demonstrate the potential by a comparison between CS, CS with thresholding or liminal CS, and two-point intensity correlation. We validate our claims by comparing the peak signal-to-noise ratio (PSNR) using CS, liminal CS, and two-point intensity correlation methods. The detailed theoretical proposition and implementation are described below.

2. TWO-POINT INTENSITY CORRELATION

A schematic of the experimental setup is shown in Fig. 1, wherein the object information represented as $E_H(\hat{r})$, scrambled by the diffuser, is Fourier transformed and captured at the observation plane. The scattered field at the observation plane is represented as

$$E_H(r) = \int E_H(\hat{r}) \exp(i\varphi(\hat{r})) \exp\left(-i\frac{2\pi}{\lambda f} r \cdot \hat{r}\right) \mathrm{d}\hat{r}, \quad (1)$$

where r and $\hat{r}$ are the position vectors on the observation and random source plane, respectively. $\varphi(\hat{r})$ is random phase introduced by the diffuser, λ is the wavelength of light, and f is focal length. The intensity $I_H = |E_H(r)|^2$ at the observation plane allows us to estimate the covariance function $C_H(r_1, r_2) = \langle \Delta I_H(r_1) \Delta I_H(r_2) \rangle$. Here $\langle \cdot \rangle$ represents ensemble average and $\Delta I_H(r_1) = I_H(r_1) - \langle I_H(r_1) \rangle$ is the spatial fluctuation in the intensity with respects to its average value. Assuming the Gaussian statistics of the random field, the fourth-order correlation can be expressed in terms of the second-order correlation $W_H(r_1, r_2) = \langle E_H^*(r_1) E_H(r_2) \rangle$ as [10]

$$C_H(r_1, r_2) = |W_H(r_1, r_2)|^2. \quad (2)$$

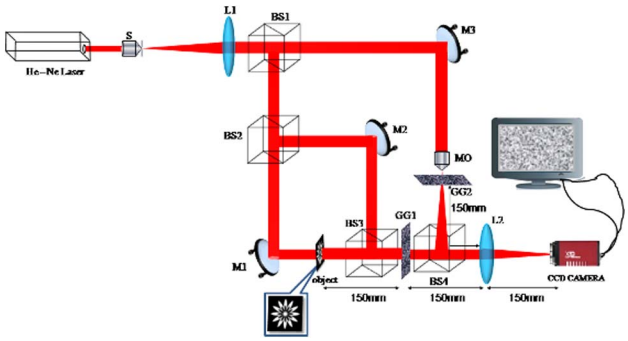

Fig. 1. Experimental configuration: S, spatial filter; BS, beam splitter; M, mirror; GG, ground glass; MO, microscope objective.

As discussed by Takeda *et al.* [9], the complex coherence function in the far field is connected to the source intensity $I_H(\hat{r})$ at the incoherent source as

$$W_H(\Delta r) = \int I_H(\hat{r}) \exp\left(-i\frac{2\pi}{\lambda f} \Delta r \cdot \hat{r}\right) \mathrm{d}\hat{r}. \quad (3)$$

Equation (3) is the Van Cittert–Zernike theorem, and term $\Delta r = r_2 - r_1$. A similar relation can also be derived for a spatially Gaussian random field [10–12].

It is observed from Eq. (2) that the phase information of the coherence function is lost while evaluating intensity correlation. Therefore, for the recovery of the object information, the lost phase of the $W_H(\Delta r)$ has to be retrieved. Recently, we have demonstrated a holographic route to recover the complex coherence function [11]. It is based on characterizing one random field, here $E_H(r)$, with *a priori* knowledge of second random field $E_R(r)$, called reference speckle. The coherent addition of two speckle fields coming from two independent diffusers, GG1 and GG2 shown in Fig. 1, at the observation plane is expressed as

$$I(r) = |E_H(r) + E_R(r)|^2. \quad (4)$$

Since diffusers used to realize object and reference fields are different, the cross correlation between these two random fields is considered to be zero, i.e., $\langle E_H^*(r_1) E_R(r_2) \rangle \approx 0$. Therefore, the covariance of the resultant speckle field is represented as

$$\langle \Delta I(r) \Delta I(r + \Delta r) \rangle = |W(\Delta r)|^2, \quad (5)$$

where $W(\Delta r) = W_H(\Delta r) + W_R(\Delta r)$. Equation (5) depicts the solution to the phase problem of the usual Hanbury Brown–Twiss (HBT) approach and is different from higher-order correlation and phase retrieval as mentioned in Ref. [11]. This coherence wave interference offers a solution to the phase problem and can be applied for imaging through random medium using Eq. (3).

In order to reconstruct the object by two-point correlation [11], we consider spatial random intensities as $I(r, m)$, with m (ranging from 1 to M) being the sequence of random fields. This can be demonstrated mathematically for the m^{th} pattern. After making the m samples (up to M), the reconstruction procedure involves cross-correlating the recorded intensity values $I(r, m)$ as shown in Eq. (6):

$$|W(r)|^2 = \frac{1}{M} \sum_{m=1}^{M} (I(0, m) - \langle I(0, m) \rangle_M)(I(r, m) - \langle I(r, m) \rangle_M). \quad (6)$$

This procedure utilizes a total of M random patterns and it involves averaging over M. As the M increases, the fidelity of the reconstruction also increases, i.e., a larger M often results in a more accurate and noise-free reconstruction. One of the ways in which this can be represented tangibly is the compression ratio N/M, where N is the total number of pixels in the computed image.

A. Experimental Configuration

To apply and compare the performance of compressive sensing in correlation holography, a setup identical to the one described for Singh *et al.* [12] is considered. Here, the ensemble average is replaced by a spatial average (rather than temporal) at the

camera plane. A brief description along with the setup is provided in Fig. 1 for better understanding. A He–Ne laser (594 nm) is spatially filtered and collimated by filtering assembly S and lens L1.

This beam is then made to pass through a beam splitter BS1 to produce two arms. The reflected arm is then further split into two by beam-splitter BS2 to produce a Mach–Zehnder interferometer. One arm of this interferometer is made to pass through the object. BS3 is then placed after the object to recombine the two arms split by BS2. The interference pattern that contains the object information is made to pass through GG1, a ground glass plane situated at a distance 150 mm away from the object, which produces a random speckle pattern (E_H). This ground glass plane simulates a scattering medium, which will hinder the direct digital recording of the object information. On the other hand, the beam transmitted by BS1 is folded by mirror M3 and focused by a microscope objective MO at an off-axis location on the ground glass GG2 in order to generate a reference random field (E_R) as described in Eq. (4). The random field coming from GG2 is also Fourier transformed by lens L2, and random fields coming from two arms are coherently superimposed and detected at the Fourier plane by a monochrome charge coupled device (CCD) (Prosilica GX2750, 2750 × 2200 pixels, and 4.54 μm pixel pitch). Different random sets (up to M) of size 300 × 300 pixels are generated from the CCD to construct a speckle data of size (2200 × 2200) pixels (at fixed time t). This framework requires a high number of samples to reconstruct the hologram; therefore, the concept of CS is applied to achieve a more effective solution.

Algorithm 1: CS Algorithmic Framework for Correlation Holography

1: Formation of Sensing Matrix ϕ:
   1. Split the speckle pattern recorded at fixed time t of size 2200 × 2200 into M small random patterns (square patches/matrices).
   2. Convert these random patterns into row vectors of dimension $1 \times N$.
   3. Stack them on each other to form a matrix of dimension $M \times N$ as shown in Fig. 2(a).
2: Formation of Measurement Vector y:
   1. Take M small random patterns (square patches/matrices).
   2. Extract the center pixel of each random patterns.
   3. Stack them on each other to form a column vector of dimension $M \times 1$ as shown in Fig. 2(b).
3: Convex Optimization:
   1. Reconstructing x from y and ϕ using Eq. (7)
   2. Reshaping x to the square patch.

3. CS FRAMEWORK FOR CORRELATION HOLOGRAPHY

The target of this paper is to propose a simple yet effective CS-based approach to emulate Eq. (6) with only few patterns.

A. Compressive Sensing Theory

The working principle of CS can be defined as the following. Let $x \in R^N$ be the signal of interest, ϕ be an $M \times N$ matrix, which is typically called a (random) sensing or measurement matrix. Let $y = \phi x$ be the M (random) measurements ($M \ll N$) of x. CS theory asserts that the signal x can be approximated from fewer measurements y provided that x is known to be k-sparse (i.e., has at most k non-zero elements) and ϕ satisfies mathematical properties such as restricted isometric property (RIP), Spark, etc. [25]. The sensing or measurement matrix usually employed for extracting the measurements is considered to be an independent and identically distributed Gaussian random matrix. This recovery problem can be formulated as follows. Given y and ϕ, recover x by minimizing $\|x\|_0$ subjected to the constraint $y = \phi x$, where $\|x\|_0$ is the 0^{th} norm (or l_0) of x (i.e., the total number of non-zero elements of x). However, this is computationally complex to perform. An alternative to l_0 norm that gives appreciably the same results is minimizing the l_1 norm, if the number of measurements $M > k \log(N/k)$. Now, the sparse recovery of x can be formulated as minimizing $\|x\|_1$ subjected to the constraint $y = \phi x$. This is usually accomplished using the convex optimization algorithms such as basis pursuit, orthogonal matching pursuit, or gradient projection sparse recovery, etc. [25,26]. In the proposed compressed correlation holography to be in-line with the two-point intensity correlation procedure, we generate sensing matrix (ϕ) and measurement matrix (y) from the same data, i.e., from experimentally detected speckle. Note that this is in contrast to compressed ghost imaging [22,23], wherein data from two detectors are used. Therefore, CS can be considered as a weighted average considering the two-point averaging between speckle patches (rows of ϕ) and their midpoints (elements of y), where the CS optimization process ensures that these weights are a sparse representation of the object; in other words, the averaging can be performed with much smaller number of speckle patches.

B. Proposed CS-Based Correlation Holography

The application of compressive sensing to correlation holography is based on the observation that a computationally efficient analogy to correlation can be accomplished by the appropriate selection of the random sensing matrix and the measurements in the context of correlation holography.

Instead of carrying out two-point correlation explicitly based on usual spatial averaging as a replacement for the ensemble average for a spatially ergodic field [Eq. (6)], we rely on the compressive sensing framework to dig through the data and present the information we want. This is based on the observation that the correlation can be recast as the (sparse) optimization problem. Specifically, the object reconstructed in two-point correlation as the (averaged) correlation between (several) speckle patches and their midpoints can be formulated as an error minimization between the product of the (vectorized) speckle patches (ϕ) and the object (x) and their midpoints (y), i.e., $\|y - \phi x\|$, while the sparse solution of this minimization problem yields efficient object reconstruction with far fewer samples.

Here we make the analogy and the formulation of each of its terms explicit for better clarity. We take the small random patterns (square patches/matrices of size 300 × 300) and reshape them into row vectors of the dimensions $1 \times N$, N being the total number of elements in each random pattern (here $N = 90,000$). Each of these M number of row vectors are

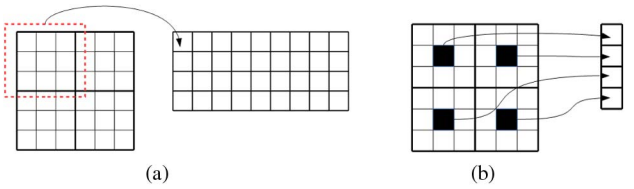

Fig. 2. (a) Schematic to show how the sensing matrix $\phi \in \mathcal{R}^{\mathcal{M}\times\mathcal{N}}$ is formed. In this case, a patch of dimensions 3 × 3 becomes a row vector of dimensions 1 × 9. (b) A schematic to show how measurement vector $y \in \mathcal{R}^{\mathcal{M}}$ is formed by stacking the center of four patches on top of each other.

then stacked on top of each other to form the sensing matrix ϕ, of the dimension $M \times N$, as shown in Fig. 2(a). Guided by two-point correlation, where the correlation between the center pixel and the patch is established explicitly, we also pick the center pixel of the M patches and stack them to construct an $M \times 1$ vector so as to implicitly establish the two-point correlation between the center and the patch through CS optimization, with M being the total number of recorded patterns, as shown in Fig. 2(b). This vector y and matrix ϕ forms our measurement vector and sensing matrix, respectively, which are needed for the CS optimization as shown in Algorithm 1. For achieving correlation through CS reconstruction, we formulate our problem as follows:

$$\min_x \|x\|_1 + \lambda\|y - \phi x\|_2, \tag{7}$$

where x is a desired column vector of dimension $1 \times N$, and λ is a Lagrange multiplier. Vector x is then reshaped into a two-dimensional square patch/image (300 × 300). This particular optimization problem is an l_1-minimization problem, which is solved using gradient projection for sparse reconstruction (GPSR).

The proposed CS framework essentially reconstructs the object that well agrees (overall correlates) with the speckle patches

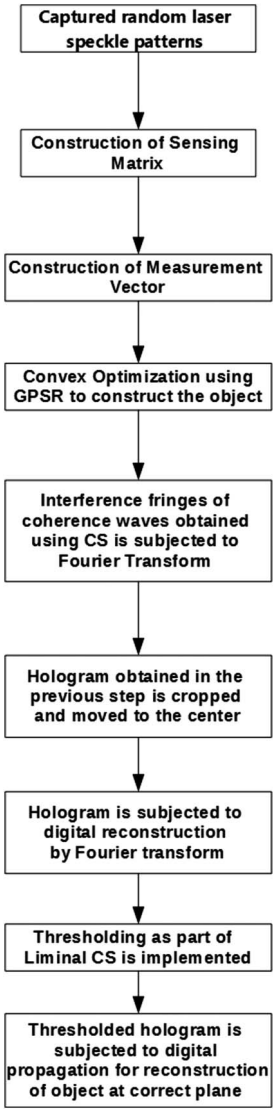

Fig. 3. Flow chart describing the CS-based algorithm.

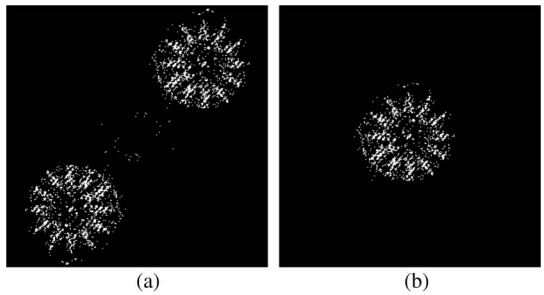

Fig. 4. (a) Fringes obtained of the first hologram using liminal CS, after performing the Fourier transform of Eq. (6). (b) The cropped version of the flower pattern in the image in Fig. 4(a).

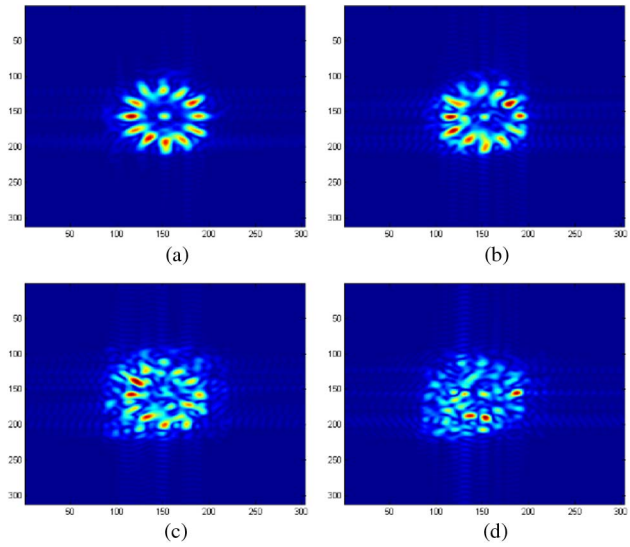

Fig. 5. (a) Final reconstruction of the object at the object plane using two-point intensity correlation (43,20,000 samples/patterns), which is taken as the reference for comparison. (b) Final reconstruction of the object on the object plane using liminal CS (16,000 samples). (c) Final reconstruction of the object on the object plane using CS (16,000 samples). (d) Final reconstruction of the object on the object plane using two-point intensity correlation (16,000 samples).

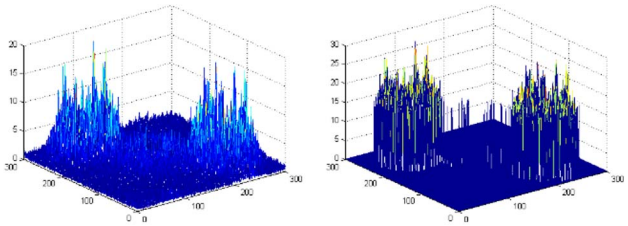

Fig. 6. (a) 3D mesh of the fringes obtained of the first hologram using CS. (b) 3D mesh of the fringes obtained of the first hologram using liminal CS.

and their midpoints. This analogy directly fits into the CS framework, as the speckle scatter matrix with which we created ϕ is random in nature and satisfies the properties like RIP, and minimizing the error $\|y - \phi x\|$ accomplishes the solution for object x that considers (midpoint) correlation between ϕ and y. This becomes midpoint correlation as y is constructed from the midpoints of speckle patches with which the columns of ϕ are created.

4. PROPOSED LIMINAL CS: IMPLEMENTATION AND EXPERIMENTATION

In order to demonstrate applicability of CS in correlation holography, we take the resultant speckle pattern for a given object. We also demonstrate that two-point correlation under the CS framework can be effectively carried out, and the random samples required for CS reconstruction of the object are far lesser than for usual two-point correlation. We further observe that slight modification in the implementation of the proposed CS approach by boosting all frequencies by adding a constant DC offset, and then thresholding improves the reconstruction performance and enables representation with even fewer samples while simultaneously denoising the reconstruction. The entire procedure of the proposed method is shown in Fig. 3, in which the first four blocks are described and implemented as discussed in Sections 2 and 3.

The reshaped matrix that we obtain after the compressive sensing recovery algorithm will contain an interference of the coherence functions $W(\Delta r) = W_H(\Delta r) + W_R(\Delta r)$. The fringe is then subjected to a Fourier transform, which shows the hologram of the object at the off-axis spectrum, as shown in Fig. 4(a).

The hologram obtained, in Fig. 4(a), is cropped out and moved to the center, as shown in Fig. 4(b). It is then again subjected to a Fourier transform, which will display the complex value and the DC component of the object at the ground-glass plane. Using the angular spectrum method, object information is propagated to $z = 150$ mm from the ground glass, and results are shown in Fig. 5(a) (43,20,000 samples) and Fig. 5(b) (16,000 samples) for two-point intensity correlation and liminal CS, respectively. It can be seen from Figs. 5(c) and 5(d) that the reconstruction at 16,000 samples is far less accurate than liminal CS.

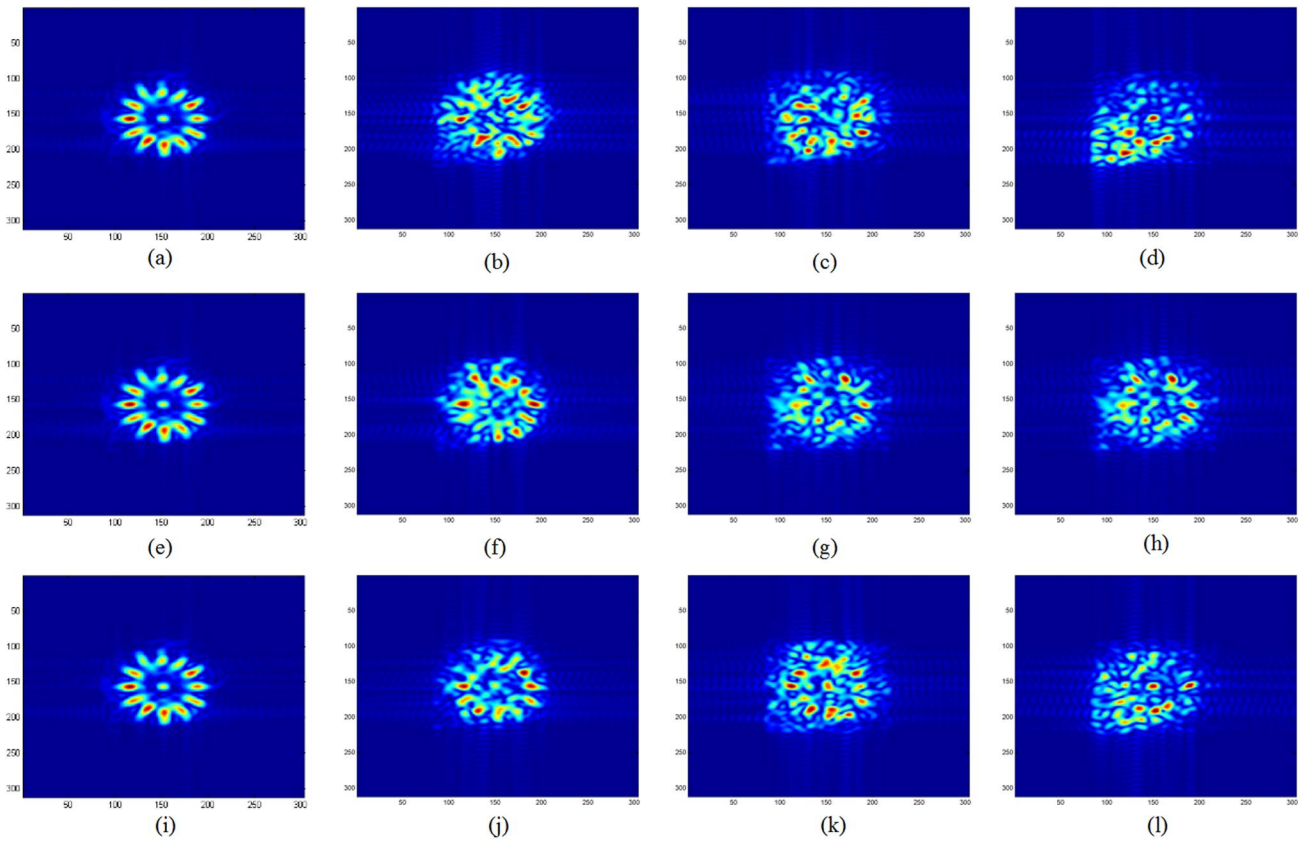

Fig. 7. Comparison of the reference (Column 1—43,20,000 samples), liminal CS framework (Column 2—5000, 7000, 11,000 samples), CS framework (Column 3—5000, 7000, 11,000 samples), and two-point intensity correlation (Column 4—5000, 7000, 11,000 samples).

Once the hologram is obtained after eliminating a DC component of the Fourier spectrum, an offset of τ is added to the image $K = \text{abs}(k) + \tau$, and adding τ boosts all the high-frequency details. Here k is the image obtained after the first Fourier transform, without the DC component. This is then subjected to a threshold ϵ. This threshold is used to denoise the hologram such that all the lower magnitude elements are eliminated, to obtain a better recovery of the hologram as shown in Fig. 6(b). We refer to this approach as liminal CS. By applying this technique, we could decrease the samples from 20,000 to 16,000 in the Compressive Sensing Framework, for a near-perfect reconstruction. Also, this has an added advantage that even with smaller samples, such as 5000 or 6000, the basic shape of the object can be obtained for the recovered hologram as shown in Fig. 7. No approach other than liminal CS can reconstruct the hologram, and with 16,000 samples it gives a near-perfect reconstruction. This technique gives a better reconstruction because it simultaneously suppresses the background of the object and boosts the object details to a higher range, hence making it more prominent in reconstruction.

We generate a plot to compare the performances of both CS-based reconstructions and the usual two-point intensity correlation method. The aim is to demonstrate the ability of liminal CS to generate a superior PSNR given an equal number of samples. PSNR is defined as the ratio between the maximum possible power of a signal and the power of corrupting noise that affects the fidelity of its representation. The mathematical definition that is used in this work is shown in Eq. (8), where R is the maximum fluctuation in the image and MSE is the mean-square error between the original image and reconstructed image:

$$\text{PSNR} = \log_{10}\left(\frac{R^2}{\text{MSE}}\right). \tag{8}$$

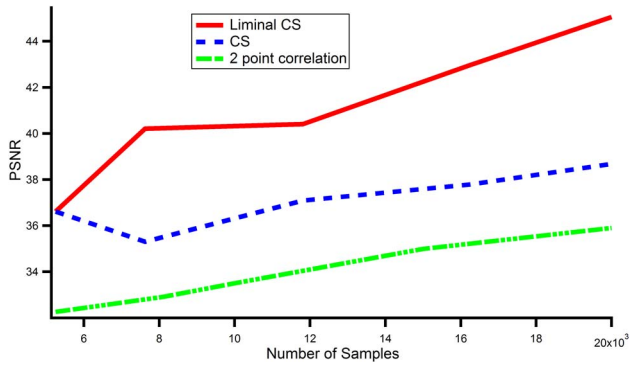

Fig. 8. Graph showing PSNR values (y axis) against the number of samples utilized for reconstruction.

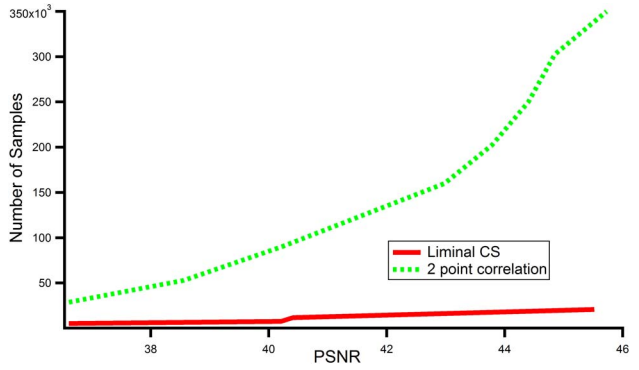

Fig. 9. Comparison of the number of samples required (in the y axis) for same PSNR (along the x axis) by two-point correlation and liminal CS.

Table 1. Time Taken to Reconstruct Using CS Framework (500 Iterations) and Two-Point Intensity Correlation

Method	Number of Samples	Time Taken
Two-point correlation	43,20,000	948 ± 5%
Liminal CS	16,000	536 ± 5%

All three methods were given a set of samples to work with, and the resulting PSNR values are plotted accordingly. As observed from Fig. 8, liminal CS has a superior PSNR, given an equal number of samples. The PSNR values are calculated by taking the reference as the image obtained by using two-point intensity correlation with all available samples (43,20,000 samples). We also show a plot comparing the number of samples required to reach a specific PSNR by liminal CS and the two-point intensity correlation method in Fig. 9. We observe that liminal CS achieves the same PSNR with significantly lesser samples. From Table 1, we infer that the time taken to reconstruct using liminal CS is significantly lesser than that of the usual two-point intensity correlation.

For a window of size 300 × 300, the number of samples considered for the two-point correlation technique is more than 1,60,000 to achieve a PSNR of 42.9. On the other hand, when liminal CS is utilized for correlation purposes for extracting qualitative phase and amplitude information from the object, we observe that for a window of the same dimensions, we can reconstruct the image easily at nearly 16,000 samples, which is 10 times less than the optimal number of samples required in the two-point correlation method.

5. CONCLUSION

In conclusion, we have successfully demonstrated the application of compressive sensing in correlation holography; the doors for future scope in correlation imaging have been thrown open. Eventually, more fields of optical imaging will be able to take advantage of the efficient nature of compressive sensing. Introduction of the CS framework reduces the number of samples, computational time, and moreover, provides high signal-to-noise ratio. The proposed technique opens the doors for possible application of compressed sensing framework for low coherent source imaging, speckle correlography, and obtaining correlation functions and coherence polarization matrices.

Funding. Department of Science and Technology, Ministry of Science and Technology (DST); Science and Engineering Research Board (SERB) (EMR/2015/00613); Indian Institute of Space Science and Technology (IIST) Trivandrum.

Acknowledgment. The authors thank Mayur Joseph for his initial contribution in this work.

REFERENCES

1. U. Schnars and W. Jueptner, *Digital Holography* (Springer, 2005).
2. I. Freund, "Image reconstruction through multiple scattering media," Opt. Commun. **86**, 216–227 (1991).
3. A. Gatti, E. Brambilla, M. Bache, and L. Lugiato, "Correlated imaging, quantum and classical," Phys. Rev. A **70**, 013802 (2004).
4. A. Gatti, E. Brambilla, M. Bache, and L. A. Lugiato, "Ghost imaging with thermal light: comparing entanglement and classical correlation," Phys. Rev. Lett. **93**, 093602 (2004).
5. O. Katz, P. Heidmann, M. Fink, and S. Gigan, "Non-invasive single-shot imaging through scattering layers and around corners via speckle correlations," Nat. Photonics **8**, 784–790 (2014).
6. J. A. Newman, Q. Luo, and K. J. Webb, "Imaging hidden objects with spatial speckle intensity correlations over object position," Phys. Rev. Lett. **116**, 073902 (2016).
7. M. J. Purcell, M. Kumar, S. C. Rand, and V. Lakshminarayanan, "Holographic imaging through a scattering medium by diffuser-aided statistical averaging," J. Opt. Soc. Am. A **33**, 1291–1297 (2016).
8. H. Li, T. Wu, J. Liu, C. Gong, and X. Shao, "Simulation and experimental verification for imaging of gray-scale objects through scattering layers," Appl. Opt. **55**, 9731–9737 (2016).
9. M. Takeda, W. Wang, Z. Duan, and Y. Miyamoto, "Coherence holography," Opt. Express **13**, 9629–9635 (2005).
10. D. N. Naik, R. K. Singh, T. Ezawa, Y. Miyamoto, and M. Takeda, "Photon correlation holography," Opt. Express **19**, 1408–1421 (2011).
11. R. K. Singh, R. Vinu, and A. Sharma, "Recovery of complex valued objects from two-point intensity correlation measurement," Appl. Phys. Lett. **104**, 111108 (2014).
12. R. K. Singh, A. M. Sharma, and B. Das, "Quantitative phase-contrast imaging through a scattering media," Opt. Lett. **39**, 5054–5057 (2014).
13. M. Takeda, A. K. Singh, D. N. Naik, G. Pedrini, and W. Osten, "Holographic correloscopy—unconventional holographic techniques for imaging a three-dimensional object through an opaque diffuser or via a scattering wall: a review," IEEE Transactions on Industrial Informatics **12**, 1631–1640 (2016).
14. M. Takeda, "Spatial stationarity of statistical optical fields for coherence holography and photon correlation holography," Opt. Lett. **38**, 3452–3455 (2013).
15. M. Takeda, W. Wang, D. N. Naik, and R. K. Singh, "Spatial statistical optics and spatial correlation holography: a review," Opt. Rev. **21**, 849–861 (2014).
16. J. Bobin, J.-L. Starck, and R. Ottensamer, "Compressed sensing in astronomy," IEEE J. Select Topics Signal Process. **2**, 718–726 (2008).
17. W. L. Chan, M. L. Moravec, R. G. Baraniuk, and D. M. Mittleman, "Terahertz imaging with compressed sensing and phase retrieval," Opt. Lett. **33**, 974–976 (2008).
18. D. J. Brady, K. Choi, D. L. Marks, R. Horisaki, and S. Lim, "Compressive holography," Opt. Express **17**, 13040–13049 (2009).
19. Y. Rivenson, A. Stern, and B. Javidi, "Overview of compressive sensing techniques applied in holography [invited]," Appl. Opt. **52**, A423–A432 (2013).
20. O. Katz, Y. Bromberg, and Y. Silberberg, "Compressive ghost imaging," Appl. Phys. Lett. **95**, 131110 (2009).
21. M. Aßmann and M. Bayer, "Compressive adaptive computational ghost imaging," Sci. Rep. **3**, 1545 (2013).
22. W. Gong and S. Han, "High-resolution far-field ghost imaging via sparsity constraint," Sci. Rep. **5**, 9280 (2015).
23. C. Zhao, W. Gong, M. Chen, E. Li, H. Wang, W. Xu, and S. Han, "Ghost imaging lidar via sparsity constraints," Appl. Phys. Lett. **101**, 141123 (2012).
24. M. I. Akhlaghi and A. Dogariu, "Compressive correlation imaging with random illumination," Opt. Lett. **40**, 4464–4467 (2015).
25. Y. C. Eldar and G. Kutyniok, *Compressed Sensing: Theory and Applications* (Cambridge, 2012).
26. M. A. T. Figueiredo, R. D. Nowak, and S. J. Wright, "Gradient projection for sparse reconstruction: application to compressed sensing and other inverse problems," IEEE J. Sel. Top. Signal Process. **1**, 586–597 (2007).